

# The Effect of Water Vapour Atmospheres on the Thermal Transformation of Kaolinite Investigated by XRD, FTIR and Solid State MAS NMR

J. Temuujin,<sup>a</sup> K. Okada,<sup>b</sup> K. J. D. MacKenzie<sup>c\*</sup> and Ts. Jadambaa<sup>d</sup>

<sup>a</sup>Institute of Chemistry of the Mongolian Academy of Sciences, Ulaanbaatar 51, Mongolia

<sup>b</sup>Department of Inorganic Materials, Tokyo Institute of Technology, O-Okayama, Meguro-ku, Tokyo 152, Japan

<sup>c</sup>New Zealand Institute for Industrial Research and Development, PO Box 31-310, Lower Hutt, New Zealand

<sup>d</sup>Department of Building Materials, Mongolian Technical University, Ulaanbaatar 46, Mongolia

(Received 27 October 1997; accepted 29 June 1998)

## Abstract

*The dehydroxylation of kaolinite and its subsequent transformation to cubic Al-spinel and mullite has been studied under water vapour atmospheres up to 0.8 atm pressure. Dehydroxylation, as determined by XRD, FTIR and solid state MAS NMR, can be accomplished at low temperatures (ca 500°C) under water vapour atmospheres, the efficiency increasing with increasing water vapour pressure. The subsequent thermal transformations to crystalline products are also facilitated by water vapour atmospheres, which also enhance the mechanical properties of the fired kaolinite (crushing strength and softening coefficient) by 3–4 times. These effects are discussed in terms of proton attack on the Si–O bonds followed by polycondensation of the resulting silanol groups to siloxane, facilitating the nucleation of mullite from amorphous aluminosilicate and strengthening the chemical bonds between the grains. © 1998 Elsevier Science Limited. All rights reserved*

**Keywords:** clays, NMR, X-ray methods, transformations, mullite

## 1 Introduction

The thermal transformation of kaolinite to mullite is of great importance to ceramic technology. One objective of investigations into the kaolinite–mullite reaction series is to find possible ways of decreasing the mullitization temperature and

increasing the amount of mullite formed during isothermal heating. In particular, the effects of grinding and reaction atmosphere on the formation of mullite from clay minerals have been studied.<sup>1–5</sup> The positive influence of water vapour atmospheres on the formation of mullite from kaolinite fired at 1100°C has been reported.<sup>4</sup> Kruglitskii and Moroz have reported<sup>6</sup> that the amount of mullite formed in a water vapour atmosphere was 3.5 times greater than that found in an oxygen atmosphere. However, in these few investigations, neither the influence of the reaction atmosphere on the processes preceding mullite formation nor the possibility of decreasing the temperature of mullite formation from kaolinite was explored. The object of the present study was to examine the effects of water vapour atmospheres on the kaolinite–mullite reaction sequence, paying particular attention to the formation and structure of the intermediate phases.

## 2 Experimental

The starting material was a Prosyranov kaolinite from the Ukraine. Its chemical composition is given in Table 1. The mineralogical impurities were quartz, a little anatase and a small amount of montmorillonite. The particle size distribution, determined for a sample ultrasonically dispersed in 0.2% aqueous sodium hexametaphosphate using a Shimadzu SALD-2001 laser interferometer, was 90% < 67 μm, 50% < 22 μm, 10% < 2.6 μm. Scanning electron microscopy (SEM) shows the grains occur in a platy/blocky morphology. The clay was used without further purification.

\*To whom correspondence should be addressed.

**Table 1.** Chemical composition of the Prosyantov kaolinite

Component	Mass %	Component	Mass %
Al <sub>2</sub> O <sub>3</sub>	38.32	SiO <sub>2</sub>	46.84
MgO	0.14	K <sub>2</sub> O	0.39
CaO	0.16	TiO <sub>2</sub>	0.78
Fe <sub>2</sub> O <sub>3</sub>	1.16	NiO	0.03
ZrO <sub>2</sub>	0.02		

Loss on ignition 13.8%.

A stiff paste was made by mixing with approximately 20% water, pressed into an open-ended cube-shaped mold of 20 mm edge length then allowed to dry to constant weight at room temperature for about 3–5 days.

Firing was carried out in the autoclave furnace shown in Fig. 1. The furnace pressure and temperature were monitored and controlled by a manometer (1) and a Pt/Rh thermocouple (3). The water vapour atmosphere was generated by a boiler (7), the required vapour pressure being kept constant by a valve (2). The cube-shaped samples were placed in the furnace and exposed to the water vapour from 400°C onwards. The samples were held for 2 h at temperatures between 500 and 800°C. After firing, the crushing strengths were measured on both dry samples, and after immersion in water for 48 h. The reported softening coefficient is the strength ratio of the wet to dry samples. Each reported strength value is based on at least 10 replicates. The fired samples were also examined by XRD, FTIR and MAS NMR. The latter measurements were made at 11.7 T using a Varian Unity 500 spectrometer with a 5 mm Doty MAS probe spun at 10–12 kHz. The <sup>29</sup>Si spectra were acquired using a 90° pulse of 6 μs and recycle delay of 60 s, and were referenced to tetramethylsilane (TMS). The <sup>27</sup>Al spectra were acquired using a 15° pulse of 1 μs and a recycle delay of 1 s, and were referenced to Al(H<sub>2</sub>O)<sub>6</sub><sup>3+</sup>.

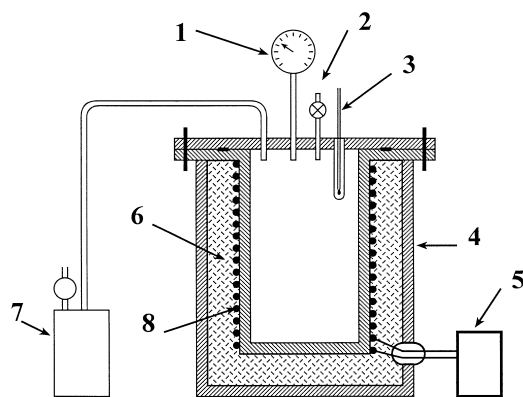


**Fig. 1.** Schematic diagram of the autoclave furnace. Key: (1) manometer, (2) pressure relief valve, (3) Pt/Rh thermocouple, (4) outer furnace jacket, (5) furnace power supply unit, (6) refractory, (7) boiler unit, (8) furnace windings.

### 3 Results and Discussion

Figure 2 shows the DTA–TG traces of Prosyantov kaolinite. The DTA trace is typical of kaolinite, showing a dehydroxylation endotherm at 513°C and exotherms at 988 and 1267°C due to the formation of spinel phase and secondary mullite respectively.

Figure 3 shows the XRD patterns of the unfired kaolinite and of samples fired at 500°C under different water vapour pressures.

The sample fired in air at this temperature (Fig. 3B) shows a slight decrease in kaolinite intensity due to the onset of dehydroxylation. By contrast, firing under increasing water vapour pressures (Fig. 3C–E) produces a progressive decrease in the kaolinite peak intensities, with the formation of the dehydroxylated phase (metakaolinite) being complete under 0.8 atm water vapour pressure. The XRD findings are fully confirmed by the FTIR measurements (Fig. 4) which show only small differences between the unfired sample and that fired in air at 500°C (Fig. 4A and B). Firing under water vapour atmospheres (Fig. 4C–E) results in the appearance of 4-coordinated Al (802 cm<sup>-1</sup>) resulting from the dehydroxylation of the kaolinite, and the disappearance of the Al–OH bands at 3622, 3651 and 3697 cm<sup>-1</sup>.

Figures 5 and 6 show the XRD and FTIR spectra of samples fired at 700 and 800°C respectively. The XRD and FTIR results for samples fired at 600°C (not shown) are similar to the 500°C results.

Samples fired in air at 700 and 800°C showed almost no evolution of the crystalline phases (Fig. 5A and B), but at 800°C, very small peaks of cubic spinel ( $\gamma$ -alumina or Al–Si spinel) were detected. Firing at 1000°C resulted in the formation of a considerable amount of spinel phase but no mullite (Fig. 5C). The sample fired at 700°C under 0.8 atm water vapour pressure (Fig. 5D) contained a large amount of spinel phase. Increasing the firing temperature to 800°C under 0.4 or 0.8 atm water vapour pressure induced mullite formation, in addition to the spinel phase (Fig. 5E and F), the intensity of the mullite peak decreasing with increased water vapour pressure.

The FTIR spectra are again in full agreement with the XRD results. Increasing the firing temperature from 700 to 800°C increases the absorption band due to 4-coordinated Al, while samples fired at 1000°C show the absorption bands at 730 and 860 cm<sup>-1</sup> arising from the 4 and 6-coordinated Al of the spinel phase.<sup>7</sup> The FTIR spectrum of the sample fired at 1000°C in air is remarkably similar to the spectrum of the sample fired in 0.8 atm water vapour at 700°C (Fig. 6D). Firing at 800°C in

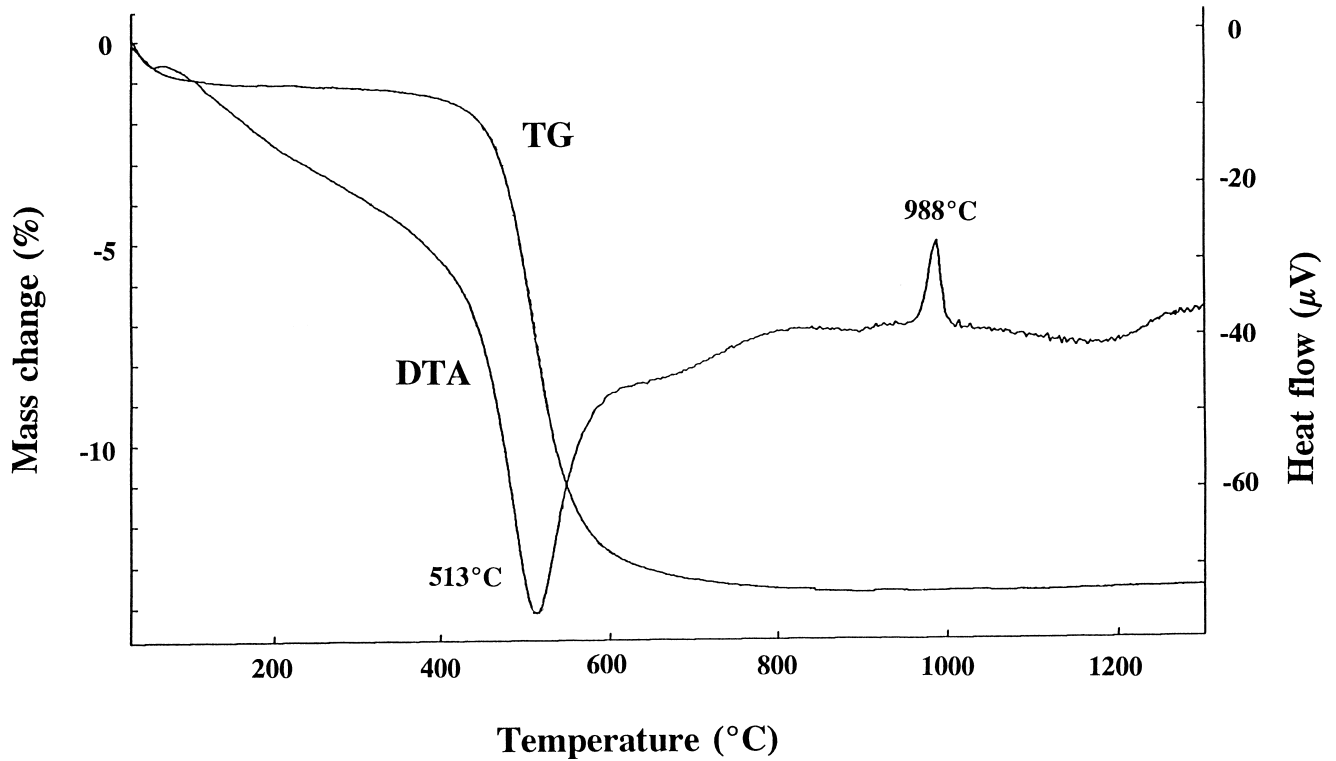


Fig. 2. DTA and TG curves for Prosyanyov kaolinite. Heating rate  $10^{\circ}\text{C min}^{-1}$  in air.

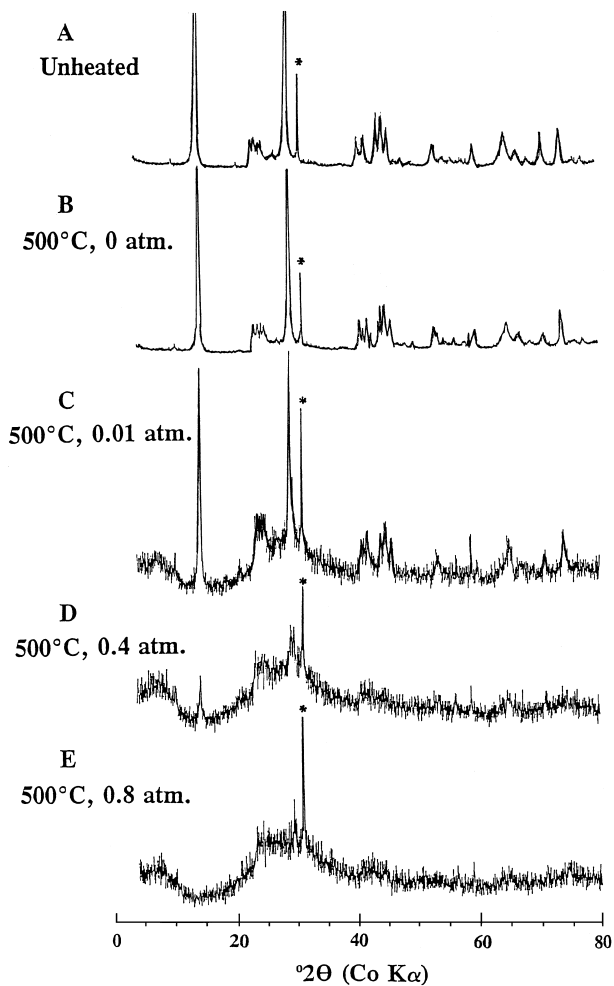


Fig. 3. XRD traces for Prosyanyov kaolinite, unheated and heated at  $500^{\circ}\text{C}$  under various water vapour atmospheres as indicated. Key: \* = quartz, unmarked peaks are kaolinite.

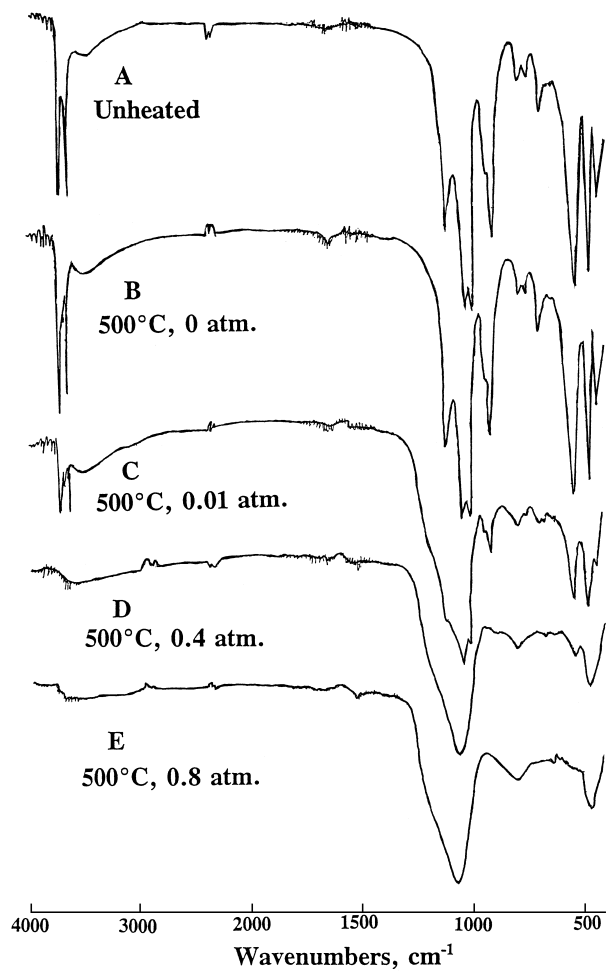


Fig. 4. FTIR spectra of Prosyanyov kaolinite, unheated and heated at  $500^{\circ}\text{C}$  under various water vapour atmospheres as indicated.

water vapour increases the absorption bands at 730 and 560  $\text{cm}^{-1}$ ; the intensities of these bands correlate with the XRD mullite intensity, since the mullite contains  $\text{AlO}_6$ ,  $\text{SiO}_4$  and isolated  $\text{AlO}_4$  groups. Samples showing strong XRD mullite intensities also clearly show the absorption bands at 730 and 560  $\text{cm}^{-1}$ .

A selection of typical  $^{27}\text{Al}$  and  $^{29}\text{Si}$  MAS NMR spectra are shown in Figs 7 and 8 respectively.

The  $^{27}\text{Al}$  spectrum of the unheated kaolinite (Fig. 7A) shows the expected single octahedral resonance at 2.4 ppm, which is unchanged by heating at 500°C in dry air. However, heating at 500°C under various water vapour pressures produces additional resonances at about 53 and 27 ppm which increase in intensity with increasing water vapour pressure (Fig. 7 B–D). These broad resonances, which are typically present in the  $^{27}\text{Al}$  spectrum of metakaolinite,<sup>8</sup> are also present in the sample dehydroxylated in dry air at 700°C (Fig. 7E). The peak at about 53 ppm corresponds to tetrahedral Al resulting from dehydroxylation, but the origin of the resonance at 27 ppm is more

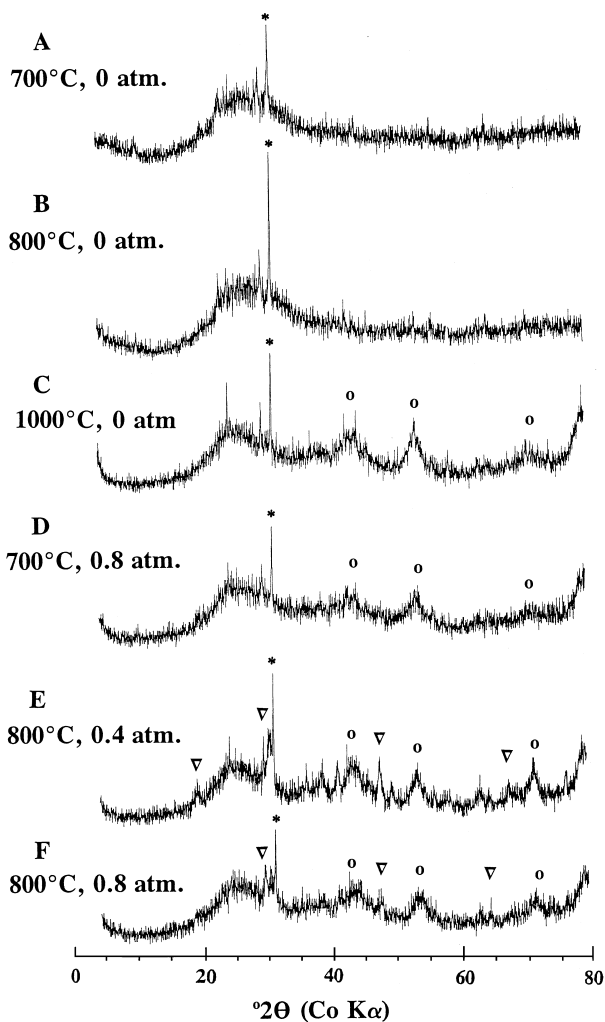


Fig. 5. XRD traces for Prosyanyov kaolinite heated at various temperatures and water vapour pressures as indicated. Key: \* = quartz, o = Al-spinel,  $\nabla$  = mullite.

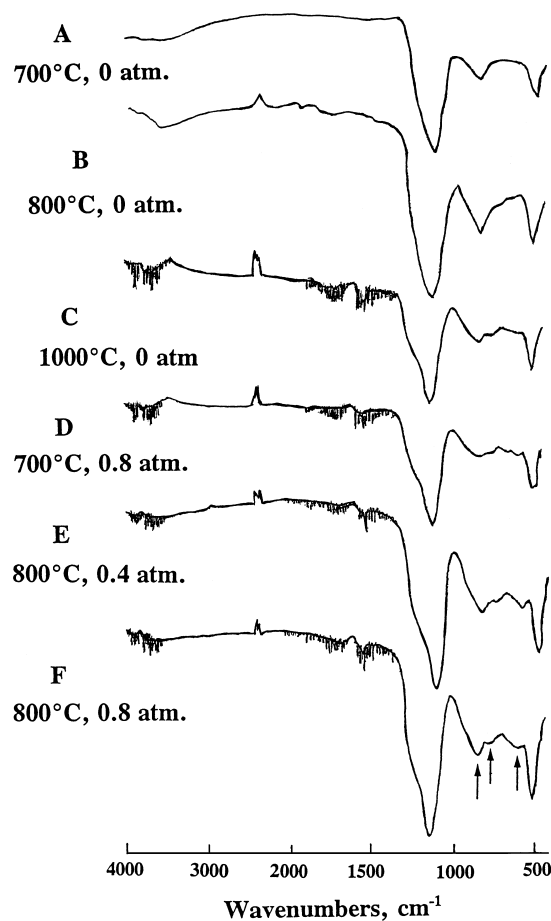


Fig. 6. FTIR spectra of Prosyanyov kaolinite heated at various temperatures and water vapour pressures as indicated.

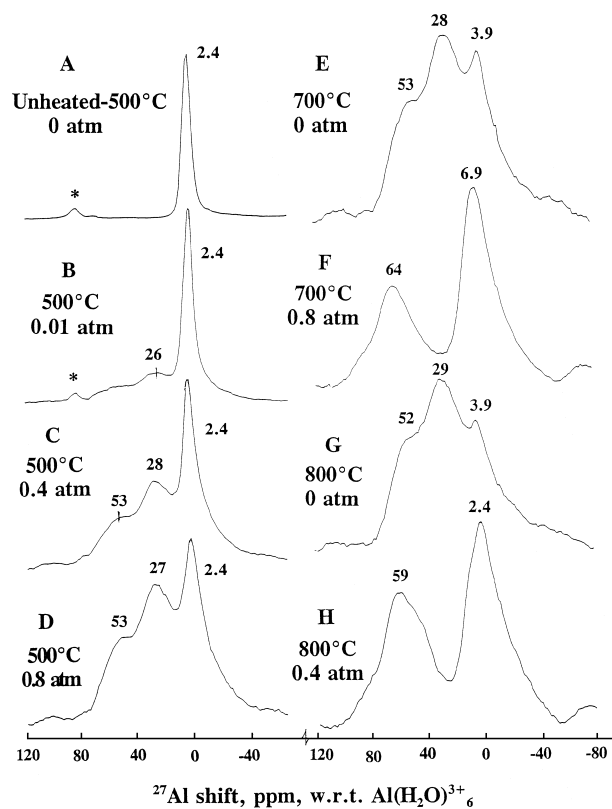


Fig. 7. 11-7 T  $^{27}\text{Al}$  MAS NMR spectra of Prosyanyov kaolinite, unheated and heated at various temperatures and water vapour pressures as indicated. Asterisks indicate spinning side bands.

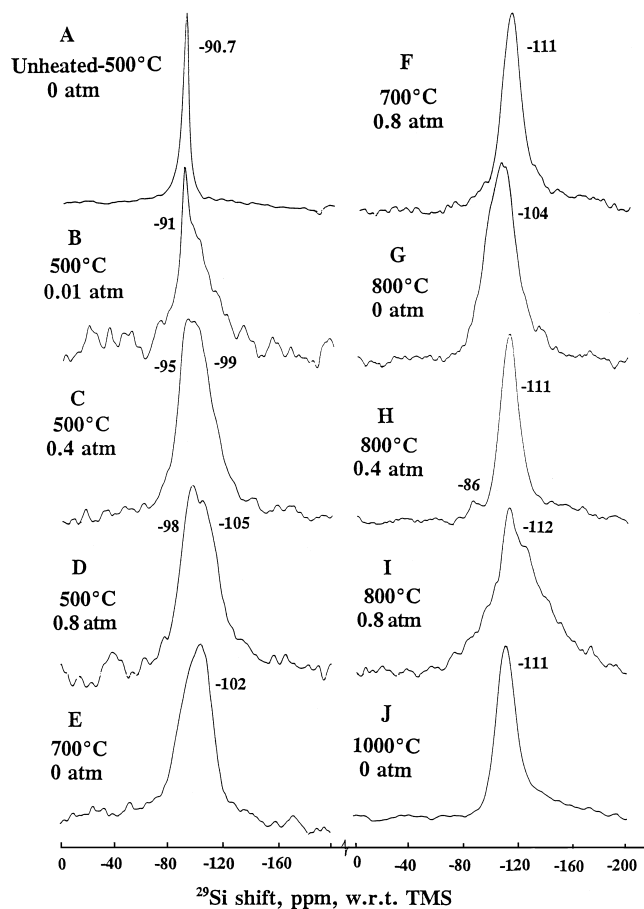


Fig. 8. 11.7 T  $^{29}\text{Si}$  MAS NMR spectra of Prosyantov kaolinite, unheated and heated at various temperatures and water vapour pressures as indicated.

open to debate, having been variously ascribed to 5-coordinated Al<sup>9</sup> or distorted 4-coordinated Al in sites which eventually form the oxygen-deficient tricluster structure characteristic of mullite.<sup>10</sup> Thus, the  $^{27}\text{Al}$  spectra are consistent with an increasing tendency for the Al sites to dehydroxylate under increasing water vapour pressures at a temperature (500°C) at which such dehydroxylation would not normally occur. The changes in the distribution of the Al over the various sites in samples heated at 500°C are shown as a function of water vapour pressure in Fig. 9.

At higher reaction temperatures (700–800°C), dehydroxylation occurs under dry conditions (Fig. 7E and G), but the presence of water vapour induces the subsequent reaction step (conversion of the metakaolinite to Al-spinel and mullite, both containing only tetrahedral and octahedral sites). This conversion is marked by the loss of the 27 ppm  $^{27}\text{Al}$  metakaolinite resonance and redistribution of the Al over the octahedral and tetrahedral sites, plotted as a function of temperature in Fig. 10 for the transformation under dry conditions.

By contrast with dry-reacted metakaolinite in which the 27 ppm peak disappears at 1000°C, the corresponding disappearance temperatures in the

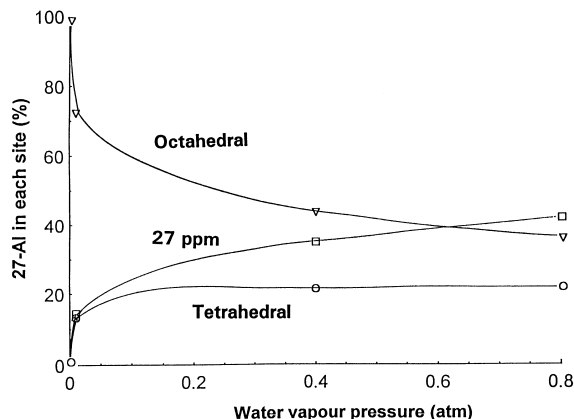


Fig. 9. Distribution of  $^{27}\text{Al}$  over the various sites of Prosyantov kaolinite heated at 500°C, as a function of water vapour pressure.

water vapour-reacted samples are lowered to 800 and 700°C under 0.4 and 0.8 atm water vapour respectively. Thus, the water vapour not only facilitates dehydroxylation, but also lowers the temperature of the subsequent reactions of the resulting metakaolinite.

The formation of a cubic spinel phase is a principal reaction in the present clay, but the shape of the tetrahedral resonance in the  $^{27}\text{Al}$  NMR spectrum at 800°C and 0.4 atm water vapour (Fig. 7H) provides evidence of enhanced mullite formation in this sample. The upfield shoulder visible in this spectrum has been attributed to the tetrahedral Al associated with the oxygen vacancy/tricluster unit of crystalline mullite.<sup>11</sup>

These conclusions are confirmed by the corresponding  $^{29}\text{Si}$  spectra (Fig. 8). The  $^{29}\text{Si}$  kaolinite resonance at  $-90.7$  ppm is retained on heating in dry air at 500°C (Fig. 8A), but in samples heated under increasing water vapour pressures, this resonance is increasingly shifted towards the metakaolinite peak position ( $-102$  ppm).<sup>12</sup> The spectra of samples heated at 500°C under increasing water vapour pressures show a splitting of this peak due

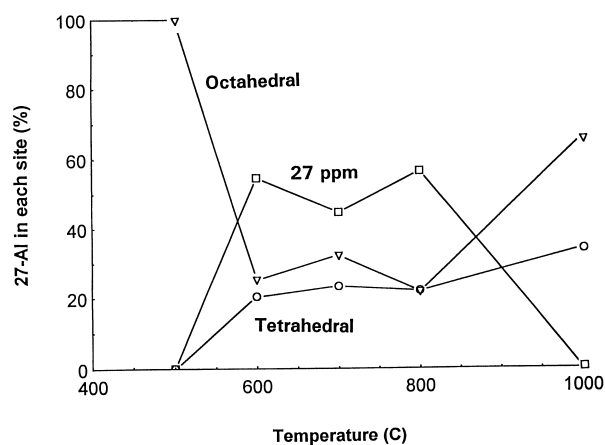
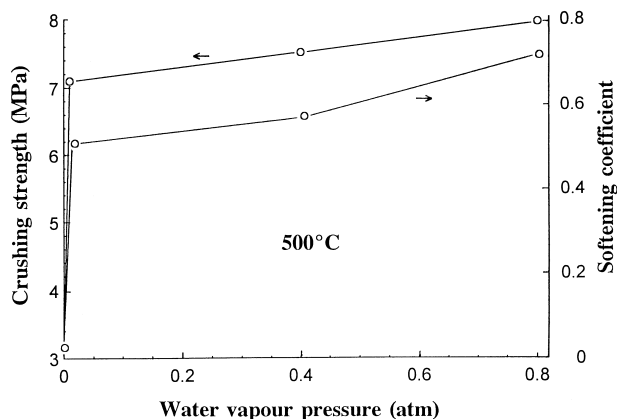


Fig. 10. Distribution of  $^{27}\text{Al}$  over the various sites in Prosyantov kaolinite heated in dry air, as a function of temperature.

to the increasing significance of the Si–OH resonance at about  $-95$  to  $-98$  ppm (Fig. 8C and D). In the samples heated at higher temperatures, the formation of new phases is accompanied by the



**Fig. 11.** Crushing strength and softening coefficient of Proyanov kaolinite heated at  $500^{\circ}\text{C}$ , as a function of water vapour pressure.

separation of amorphous silica which appears at  $-111$  ppm.<sup>12</sup> The small amount of Si which may be incorporated in the cubic spinel phase forms part of the broad  $^{29}\text{Si}$  resonance envelope, but has been previously detected only in samples from which the

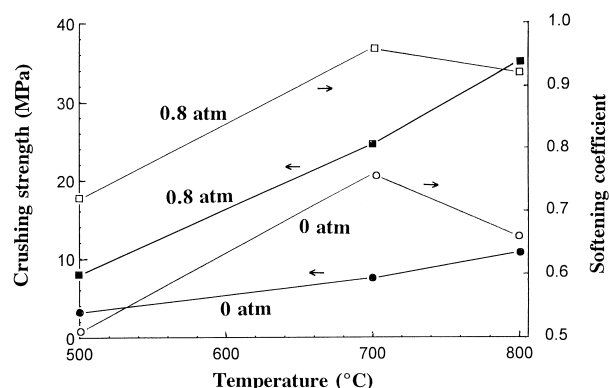


**Fig. 12.** Crushing strength and softening coefficient of Proyanov kaolinite heated under dry conditions and  $0.8$  atm water vapour pressure, as a function of temperature.

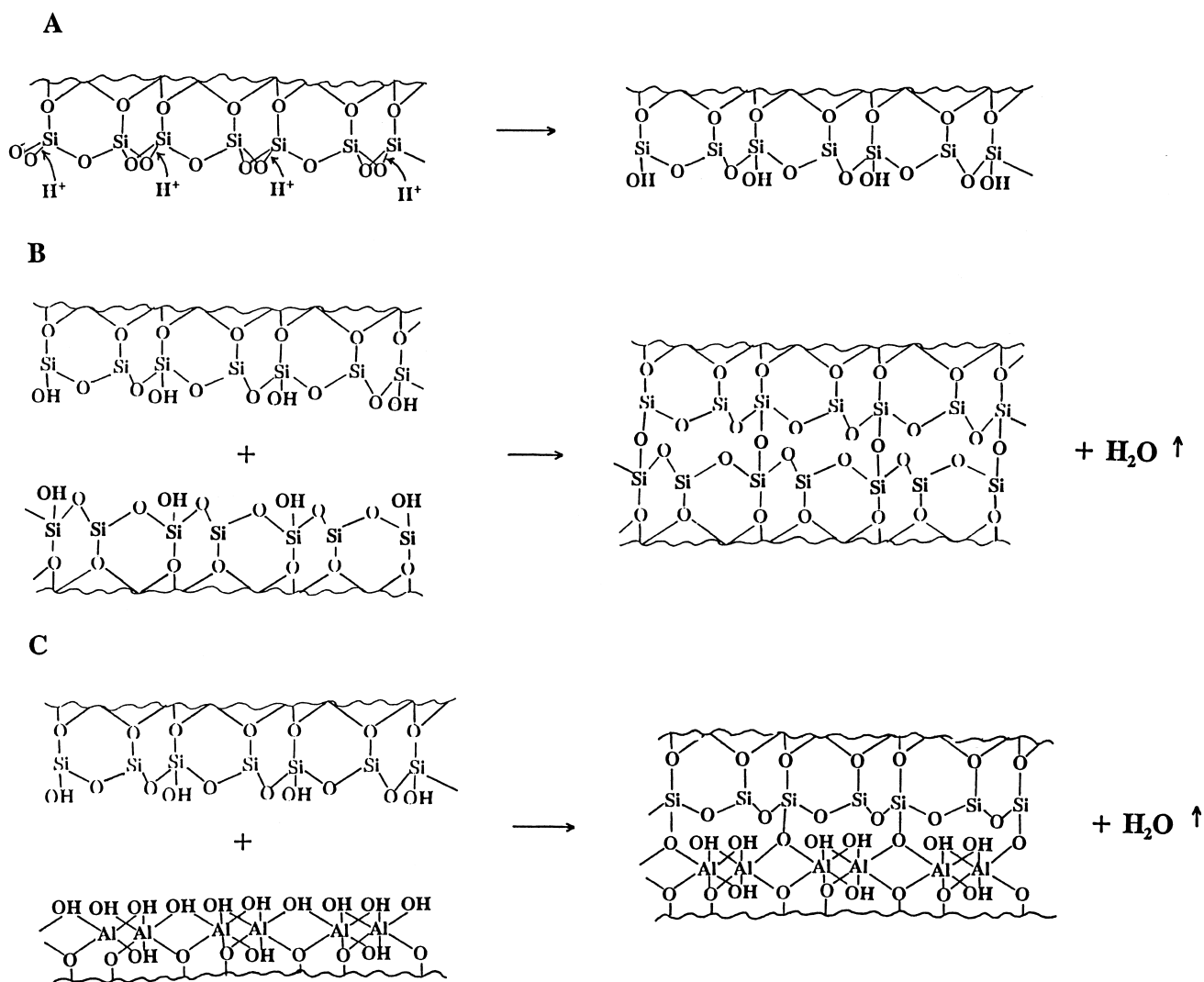


**Fig. 13.** Schematic diagram, based on the computer-generated kaolinite structure, of (A) Proton attack on the tetrahedral Si kaolinite layer with the formation of -olo- bonds, (B) Polycondensation between the -olo- bonds of the Si tetrahedral layers of different kaolinite plates, (C) Polycondensation between the -olo- bonds of the Si tetrahedral layer and the Al–OH polyhedral layers of different kaolinite plates.

uncombined amorphous silica was leached.<sup>13</sup> However, the presence of mullite after treatment at 800°C and 0.4 atm water vapour pressure is confirmed by the characteristic resonance at -86 ppm (Fig. 8H). At this temperature, higher water vapour pressures were found to decrease the XRD mullite intensity; the broad, tailing shape of the corresponding <sup>29</sup>Si spectrum (Fig. 8I) suggests that under such highly humid conditions, a continuum of Si-Al species is present, possibly signifying the hydrothermal formation of a range of less crystalline hydrous aluminosilicates.

Firing in a water vapour atmosphere also increases the mechanical strength of the samples and softening coefficient (ratio of wet to dry crushing strengths) of the samples. At 500°C, a large increase in both these parameters occurs at 0.01 atm water vapour pressure, with more modest

increases at higher vapour pressures (Fig. 11). The crushing strength of samples fired in dry atmospheres increases slightly with temperature from 3.2 MPa at 500°C to 10.74 MPa at 800°C, but under 0.8 atm water vapour pressure, the crushing strength increases over the same temperature range from 10.7 to 35.2 MPa (Fig. 12).

Similar enhancement of the physical properties (hardness and crushing strength) have been reported in kaolinite fired under applied electric fields, especially at the negative electrode;<sup>14,15</sup> this effect was explained in terms of the migration of protons to that electrode, resulting in a higher concentration of water vapour in that region. A possible explanation for the enhancing effect of humid atmospheres might be as follows:

Under humid conditions, particularly with increasing water vapour pressure, the water will attack the Si-O bonds, forming Si-OH groups (shown schematically in Fig. 13A). The formation of -olo- bonds at the tetrahedral Si faces of the kaolinite plates increases the possibility of polycondensation of the grains, between either the tetrahedral Si-OH faces (Fig. 13B) or the polyhedral Al-OH faces of different grains (Fig. 13).

The increased strength results from stronger chemical bonding between the grain contacts, achieved in the absence of a liquid phase as shown schematically in Fig. 14.

The formation of -olo- bonds rather than -oxo- bonds is also implicated in mullite formation.

After the formation of the spinel phase with the segregation of silica, the presence of -olo- bonds may facilitate the nucleation of mullite from amorphous aluminosilicate, or on the surface of  $\gamma$ -Al<sub>2</sub>O<sub>3</sub> into which silica is incorporated.

#### 4 Conclusions

Water vapour atmospheres enhance the dehydroxylation of kaolinite to form metakaolinite; the effect, as evidenced by the intensity of the 27 ppm <sup>27</sup>Al resonance, increases with increasing water vapour pressure. Formation of cubic Al-spinel and mullite at higher temperatures is also facilitated by water vapour atmospheres, the transformation temperature being lowered from 1000°C in dry conditions to 800 and 700°C under water vapour pressures of 0.4 and 0.8 atm respectively. The mechanical properties of kaolinite fired under water vapour atmospheres are also improved. These effects are ascribed to proton attack on the Si-O bonds forming silanol groups which can condense to form siloxane, resulting in stronger chemical bonding between the grain contacts even in the absence of a liquid phase.

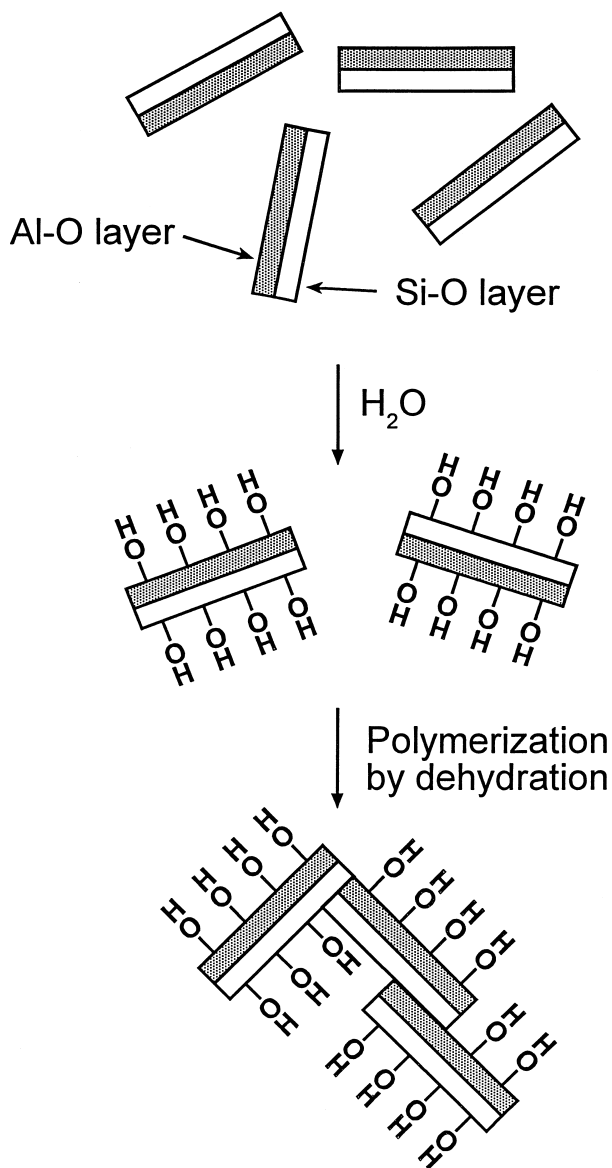


Fig. 14. Schematic diagram of strength development in kaolinite compacts by formation of -olo- groups in a humid atmosphere followed by polymerisation to form strongly bonded aggregates.

## References

1. Kawai, S., Yoshida, M. and Hashizume, G., Preparation of mullite from kaolin by dry-grinding. *Nippon Seramikkusu Kyokai Gakujutsu Ronbunshu*, 1990, **98**, 669–674.
2. Okada, K., Otsuka, N. and Ossaka, J., Structural change of allophane by dry grinding and its influence on the allophane-mullite thermal sequence. *Clay Sci.*, 1987, **6**, 283–294.
3. Sanchez-Soto, P. J., Perez-Rodriguez, J. L., Sobrados, I. and Sanz, J., Influence of grinding in pyrophyllite-mullite thermal transformation assessed by  $^{29}\text{Si}$  and  $^{27}\text{Al}$  MAS NMR spectroscopies. *Chem. Mater.*, 1997, **9**, 677–684.
4. MacKenzie, K. J. D., The effects of impurities on the formation of mullite from kaolinite-type minerals. III. The effect of the firing atmosphere. *Trans. Brit. Ceram. Soc.*, 1969, **69**, 103–109.
5. MacKenzie, K. J. D., Meinhold, R. H., Brown, I. W. M. and White, G. V., The formation of mullite from kaolinite under various reaction atmospheres. *J. Eur. Ceram. Soc.*, 1996, **16**, 115–119.
6. Kruglitskii, N. K. and Moroz, V. I., *Isskustvennie Silikaty*, Kiev, *Naukovo Dumka*, 1986, p. 220.
7. Percival, H. J., Duncan, J. F. and Foster, P. K., Interpretation of the kaolinite-mullite reaction sequence from infrared absorption spectra. *J. Amer. Ceram. Soc.*, 1974, **57**, 57–61.
8. Meinhold, R. H., Slade, R. C. T. and Davies, T. W., High-field  $^{27}\text{Al}$  MAS NMR studies of the formation of metakaolinite by flash calcination of kaolinite. *Appl. Magn. Reson.*, 1993, **4**, 141–155.
9. Lambert, J. F., Millman, W. S. and Fripiat, J. J., Revisiting kaolinite dehydroxylation: a  $^{29}\text{Si}$  and  $^{27}\text{Al}$  MAS NMR study. *J. Amer. Chem. Soc.*, 1989, **71**, C418–C421.
10. Schmücker, M. and Schneider, H., A new approach on the coordination of Al in non-crystalline gels and glasses of the system  $\text{Al}_2\text{O}_3\text{-SiO}_2$ . *Ber. Bunsenges. Phys. Chem.*, 1996, **100**, 1550–1553.
11. Merwin, L. H., Sebal, A., Rager, H. and Schneider, H.,  $^{29}\text{Si}$  and  $^{27}\text{Al}$  MAS-NMR spectroscopy of mullite. *Phys. Chem. Mineral.*, 1991, **18**, 47–52.
12. MacKenzie, K. J. D., Brown, I. W. M., Meinhold, R. H. and Bowden, M. E., Outstanding problems in the kaolinite-mullite reaction sequence investigated by  $^{29}\text{Si}$  and  $^{27}\text{Al}$  solid-state nuclear magnetic resonance. *J. Amer. Ceram. Soc.*, 1985, **68**, 293–297.
13. MacKenzie, K. J. D., Hartman, J. S. and Okada, K., MAS NMR evidence for the presence of silicon in the alumina spinel from thermally transformed kaolinite. *J. Amer. Ceram. Soc.*, 1996, **79**, 2980–2982.
14. MacKenzie, K. J. D., Effect of high-temperature direct-current electrolysis on properties of hydrous aluminosilicates. *J. Appl. Chem.*, 1971, **20**, 80–86.
15. MacKenzie, K. J. D., The influence of A.C. and D.C. electric fields on the high-temperature reactions of aluminosilicates. *Proc. Brit. Ceram. Soc.*, 1971, **19**, 202–227.